

## Effect of Synthetic Peptides Belonging to E2 Envelope Protein of GB Virus C on Human Immunodeficiency Virus Type 1 Infection

Elena Herrera,<sup>†</sup> Solveig Tenckhoff,<sup>‡</sup> María J. Gómara,<sup>†</sup> Ramona Galatola,<sup>†</sup> María J. Bleda,<sup>†</sup> Cristina Gil,<sup>||</sup> Guadalupe Ercilla,<sup>⊥</sup> José M. Gatell,<sup>||,⊥</sup> Hans L. Tillmann,<sup>‡,§</sup> and Isabel Haro<sup>\*,†</sup>

<sup>†</sup>Unit of Synthesis and Biomedical Applications of Peptides (IQAC-CSIC), Barcelona, Spain, <sup>‡</sup>Faculty of Medicine, University of Leipzig, Leipzig, Germany, <sup>§</sup>GI/Hepatology Research Program, Division of Gastroenterology, Duke Clinical Research Institute, Duke University, Durham, North Carolina, <sup>||</sup>AIDS-Research Group, IDIBAPS, Barcelona, Spain, and <sup>⊥</sup>Services of Infectious Diseases and Immunology, Hospital Clinic Barcelona, University of Barcelona, Spain

Received April 13, 2010

The use of synthetic peptides as HIV-1 inhibitors has been subject to research over recent years. Although the initial therapeutic attempts focused on HIV-coded enzymes, structural HIV proteins and, more specifically, the mechanisms that the virus uses to infect and replicate are now also considered therapeutic targets. The interest for viral fusion and entry inhibitors is growing significantly, given that they are applicable in combined therapies or when resistance to other antiretroviral drugs is seen and that they act before the virus enters the cell. The 124 synthetic sequences of the GBV-C E2 envelope protein have been obtained by SPPS. The interaction of certain GBV-C peptide sequences with the HIV-1 fusion peptide has been proven through the use of biophysical techniques. We also show how GBV-C E2 domains notably decrease cellular membrane fusion and interfere with the HIV-1 infectivity in a dose-dependent manner, highlighting their potential utility in future anti-HIV-1 therapies.

### Introduction

When a supposedly new hepatitis virus, the GB virus C (GBV-C<sup>a</sup>), also known as the hepatitis G virus (HGV),<sup>1,2</sup> was discovered in the mid-1990s, many research groups sought to correlate it to hepatic inflammation or other associated diseases. However, no impact on health<sup>3,4</sup> could be identified until the research group of Prof. Tillmann demonstrated GBV-C viraemia to be associated with significant survival benefit in HIV-infected patients.<sup>5</sup> These results were subsequently confirmed by this and other research groups.<sup>6,7</sup> Although the results were sometimes not clearly significant,<sup>8</sup> a meta-analysis underlined GBV-C's association with a more beneficial course of disease.<sup>9,10</sup>

Several mechanisms seem to be involved in the beneficial effect: down-regulation of HIV co-receptors (C–C chemokine receptor type 5 (CCR5) and CXCR4), the induction of natural ligands for these chemokine receptors (regulated on activation normal T expressed and secreted (RANTES), macrophage inflammatory protein 1  $\alpha$  and  $\beta$  (MIP-1 $\alpha$  and MIP-1 $\beta$ ), stromal derived factor 1 (SDF-1)),<sup>11,12</sup> and decrease of Fas-induced lymphocyte apoptosis, the expression of which is higher in HIV-infected patients.<sup>13</sup>

Recently it has been shown that two GBV-C proteins inhibit HIV replication in vitro.<sup>14,15</sup> Thus, there is evidence for a casual relation of GBV-C and a more prolonged survival rate in patients co-infected with GBV-C and HIV.

It was further demonstrated that some effects can be achieved by two different GBV-C proteins: the envelope glycoprotein E2 inhibits R5 and X4-tropism HIV isolates by decreasing the surface expression of CCR5 co-receptors and inducing RANTES, one of the three known ligands for CCR5. The mechanism by which E2 inhibits the X4 virus has not been fully classified, although results point to the fact that the E2 protein of the GBV-C inhibits stages prior to replication, such as the binding or fusion of membranes. The second protein proposed by Prof. Stapleton's group is the nonstructural GBV-C NS5A. The NS5A protein decreases the surface expression of CXCR4 and increases the release of SDF-1, the CXCR4 ligand, in cell culture supernatants.<sup>16</sup> Furthermore, this group classified the peptide requirements of the GBV-C NS5A protein involved in HIV inhibition through mutagenesis and proved that synthetic peptides are capable of reproducing the effects of NS5A peptides expressed intracellularly, suggesting the use of these synthetic peptide sequences from a therapeutic stance.<sup>17</sup>

Though peptides have the disadvantage of requiring parenteral application, effective peptides are better than no further treatment option, as in the setting of resistance to several oral agents. HIV-1-inhibiting peptides have been identified and/or developed using different methods. Some therapeutic peptides such as enfuvirtide, already approved for clinical use,<sup>18</sup> are derived from the HIV-1, whereas others are natural peptides such as the chemokines, defensins, or the "virus inhibitory peptide" (VIRIP)<sup>19</sup> or have been designed and synthesized

\*To whom correspondence should be addressed. Phone: +34934006109. Fax: +34932045904. E-mail: isabel.haro@iqac.csic.es.

<sup>a</sup> Abbreviations: FP, fusion peptide; GBV-C, GB virus C; HGV, hepatitis G virus; HIV-1, human immunodeficiency type 1; IC<sub>50</sub>, half maximal inhibitory concentration; ITC, isothermal titration calorimetry; LUV, large unilamellar lipid vesicles; moi, multiplicity of infection; PBMC, peripheral blood mononuclear cell; SPPS, solid phase peptide synthesis; SPR, surface plasmon resonance; TCID<sub>50</sub>, 50% tissue culture infective dose; VIRIP, virus inhibitory peptide.

## E2 (U45966\_USA)

APASVLGSRPFYGLTWQSCSCRANGSRYYTTEKGVWDRGNVTLCCDCPNPWPV  
 WLPAFCQAIGWGDPIHWSHGQNRWPLSQCQYVYGSVSVTCVWGSVSWFASTG  
 GRDSKIDVWSLVVPGVSASCTIAALGSSDRDVTVELSEWGVPCATCILDRRPASC  
 TCVRDCWPETGSRVRFPHRCGAGPKLTKDLEAVPFVNRRTPTFTIRGLPNQGRGN  
 PVRSPGFGSYAMTKIRDLSHLVKCPTPAIEPTGTGFFPGVPLNCLLLGTEVS  
 EALGGAGLTGGFYELVRRRSELMGRNPNVCPGFAWLLSSGRPDGFIHVQGHLE  
 VDAGNFIPPRWLLDFVFLLYLMLKLAEARLVPLILLLLWWWVNLAVLGLPA  
 VDAAVA

**Figure 1.** Primary sequence of E2 GBV-C protein.

from crystallographic data on HIV-1 proteins or from peptide libraries.<sup>20</sup> Furthermore, understanding the mechanism of how GBV-C E2 protein inhibits HIV might open other avenues of treatment for this devastating disease.

At present, the interest for viral fusion and entry inhibitors is growing significantly,<sup>21</sup> given that they are applicable in combined therapies or when resistance to other antiretroviral drugs is seen and that they act before the virus enters the cell, which could have the same potential as the inducing of immunity provided by a vaccine. In our group, synthetic sequences of the GBV-C E2 envelope protein have been obtained by solid-phase peptide synthesis (SPPS). The interaction of certain GBV-C peptide sequences with the HIV-1 fusion peptide has been proven through the use of biophysical techniques such as circular dichroism, Fourier transform infrared spectroscopy, isothermal titration calorimetry, and <sup>1</sup>H nuclear magnetic resonance.<sup>22</sup>

In the present article we show how certain E2 domains interfere with the HIV-1 fusion peptide-vesicle interaction and notably decrease cellular membrane fusion and interfere with the HIV-1 infectivity in a dose-dependent manner, highlighting a potential utility of some peptides in future anti-HIV-1 therapies.

## Results

**Biophysical Characterization of GBV-C Peptides/FP gp41 HIV-1 Interaction.** In order to study the possible interaction of the envelope protein E2 with the fusion peptide (FP) of glycoprotein gp41 of the HIV-1 virus during the entry process of the virus into the cell, a scan of this glycoprotein was carried out by means of the synthesis of peptide sequences of 18 amino acids overlapped in 15 residues. The best preserved primary structure of the E2 protein taken from the Genbank database is shown in Figure 1, and multiple syntheses were carried out in parallel to obtain 124 peptides corresponding to this protein. All peptides were characterized using high performance liquid chromatography (HPLC) and HPLC-mass spectrometry (HPLC-MS) and showed purity greater than 90% (Table 1 in Supporting Information).

These peptides were evaluated in regard to their capacity to inhibit the destabilization process of lipid vesicles induced by the HIV-1 FP. As shown in Figure 2, the peptides P45–P46, P59, and P97 inhibit the leakage induced by the HIV-1 FP at a relationship of 1/10 (FP/E2 peptide) in an extent higher than 50%, with P11, P40–41, P80–82, P88–P91, P96, P105–P109, and P124 peptide regions also being capable of inhibiting the activity of the HIV-1 FP

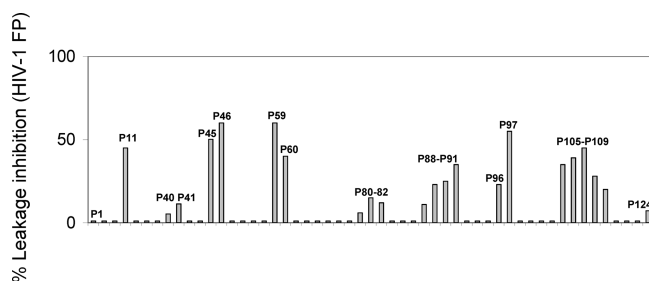


**Figure 2.** Inhibitory effect of the E2 GBV-C overlapped peptides on the HIV-1 FP induced leakage assay.

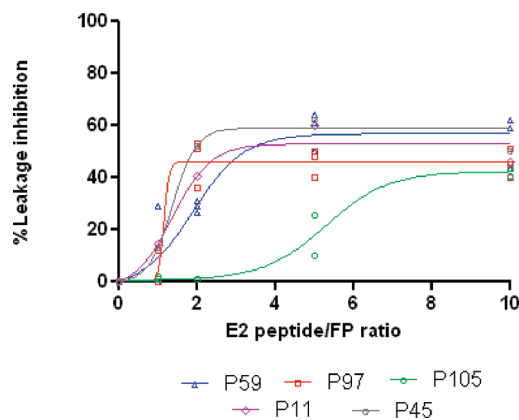


**Figure 3.** Inhibitory effect on HIV-1 FP induced leakage of P59, P97, P105, P11, and P45 E2 peptides. The extent of leakage inhibition was plotted as a function of the P<sub>x</sub>/HIV-1 FP molar ratio.

**Table 1.** Area under the Curve and Coordinates of the Peak for the Inhibitory Effect on HIV-1 FP Induced Leakage of P11, P45, P59, P97, and P105 E2 Peptides

	P11	P45	P59	P97	P105
area under the curve	449.8	491.7	438.0	394.7	180.6
% Inhibition for E2 Peptide/FP Ratio of 5					
Y = % inhibition	52.9	59.0	56.3	46.0	17.9

although to a lower extent. The intrinsic lytic effect of the GBV-C peptides alone was null or negligible.

To confirm the anti-HIV-1 FP activity observed and thus to exclude the possibility that a contaminating agent might be responsible for the observed effects of E2 peptides, we next resynthesized manually and purified by preparative HPLC the selected peptides. Further experiments confirmed the inhibitory capacity of the selected E2 18-mer peptides.

Several ratios of the HIV-1 FP and the P11, P45, P59, P97, and P105 (1:1, 1:2, 1:5, and 1:10) were tested in leakage assays. As shown in Figure 3, these peptides inhibit the permeabilization vesicular process induced by the HIV-1 FP, the percentage of inhibition for a E2 peptide/HIV-1 FP ratio being higher for P45 (Table 1). The plateau observed during the leakage assay was in all cases lower than 65%. Despite an increase of the E2 peptides/HIV-1 FP ratio, the total inhibition of the permeabilization process induced by HIV-1 FP was not observed.

In order to test the specificity of the interaction between the E2 peptides and HIV-1 FP, we used melittin as a control peptide. Melittin induced 8-aminonaphthalene-1,3,6-trisulfonic acid, disodium salt (ANTS), and *p*-xylenebispiridinium bromide (DPX) leakage from palmitoyllecithin phosphatidylglycerol (POPG) large unilamellar lipid vesicles (LUVs) at

peptide-to-lipid mole ratios higher than  $1/50$ . The 50% of POPG vesicular content leakage induced by melittin was established at a peptide-to-lipid mole ratio of  $1/10$ . When the assay was performed in the same conditions as using the HIV-1 FP, a relationship of  $1/10$  of melittin/E2 peptides was premixed in dimethyl sulfoxide (DMSO) and tested in the leakage assay (data not shown). The results showed that E2 peptides were unable to inhibit the membrane lytic activity of melittin, thus indicating the specificity of the interaction between GBV-C E2 peptides and the HIV-1 FP.

The interactions of E2 peptides with HIV-1 FP were examined by measuring their partitioning in POPG liposomes. As shown in Figure 4A, relative to fluorescence in buffer, the maximum wavelength of Trp emission ( $\lambda_{\text{max}}$ ) of HIV-1 FP shifted dramatically toward the blue in the presence of 75  $\mu\text{M}$  POPG LUV. Specifically  $\lambda_{\text{max}}$  decreased by more than 20 nm consistent with the movement of HIV-1 FP into a nonpolar environment of vesicles bilayers. The

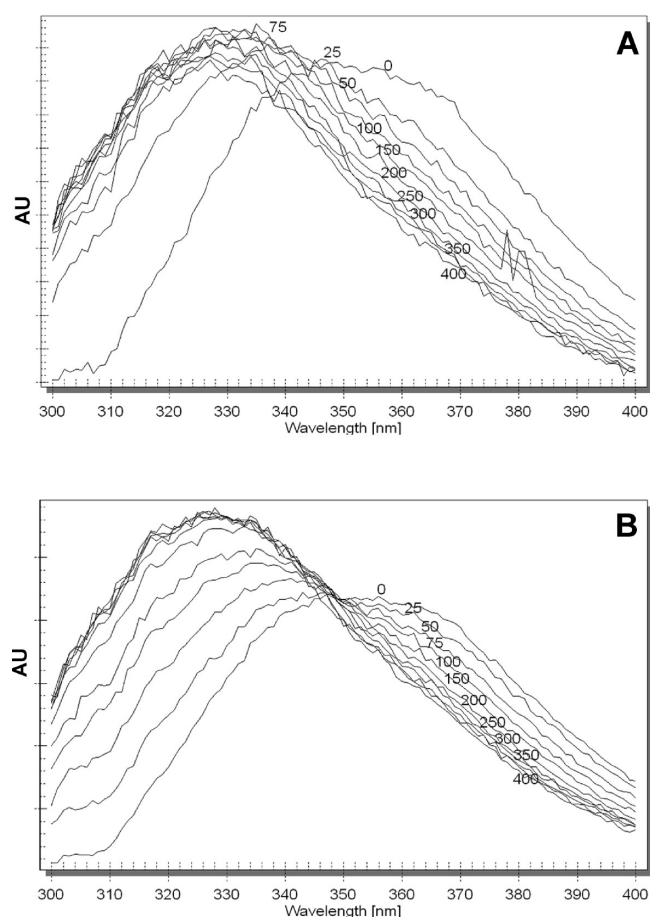


**Figure 4.** Fluorescence emission spectra of (A) FP and (B) equimolar mixture of FP and p97 upon titration with POPG LUVs. FP concentration is 2  $\mu\text{M}$ .

incubation of E2 peptides with HIV-1 FP in an equimolar ratio prior to the POPG titration notoriously avoids the shift of the Trp emission fluorescence, thus indicating an interaction of E2 peptides with HIV-1 FP that prevents the movement of the Trp residue to an environment of lower polarity provided by the vesicles. As an example, in Figure 4B we show the fluorescence emission spectra of an equimolar mixture of HIV-1 FP and P97.

Fluorescence titration was used to measure HIV-1 partitioning quantitatively by measuring fluorescence intensity at the  $\lambda_{\text{max}}$  (327 nm). The partitioning isotherms (Figure 1 in Supporting Information) show that HIV-1 FP partitioned strongly into POPG vesicles ( $K_x = (9.7 \pm 1.7) \times 10^5$ ). The mole fraction partition coefficients ranged from  $(1.7 \pm 0.4) \times 10^5$  for HIV-1 FP/P59 to  $(7.5 \pm 0.8) \times 10^5$  for HIV-1 FP/P105, with P59 and P97 thus being the GBV-C E2 peptides that more efficiently prevented the HIV-1 FP binding to the POPG vesicles and with P105 being the less active peptide in this assay.

To quantify the interaction of E2 peptides with the HIV-1 FP, we performed surface plasmon resonance (SPR) and isothermal titration calorimetry (ITC) studies. We used a Biacore T-100 SPR biosensor to screen the direct interactions of E2 peptides to HIV-1 FP. The kinetic binding parameters and equilibrium constants for the peptides are given in Table 2. Results obtained using immobilized HIV-1 FP and the selected E2 synthetic peptides as analytes showed a clear interaction between P11, P45, P97, and P105 and the HIV-1 FP, the  $K_D$  values being between  $2.24 \times 10^{-6}$  and  $5.86 \times 10^{-5}$  M. Of note is that the dissociation constant of P97 was 1 order of magnitude lower. Between 30- and 100-fold faster associations were observed for P97 compared to P11, P45, and P105. Figure 5 shows as an example the adjusted sensorgram for the P105 peptide.

The values for the binding affinities to HIV-1 FP were validated by ITC. Figure 6 shows ITC results where HIV-1 FP was titrated with P11. The ITC experiments yielded  $K_D$  values of  $3.3 \times 10^{-5}$ ,  $6.3 \times 10^{-5}$ ,  $3.9 \times 10^{-6}$ , and  $2.0 \times 10^{-5}$  M for P11, P45, P97, and P105, respectively, in excellent agreement with the values determined by SPR. The very low interaction observed for P59 could not be fitted into any of the defined binding models. Then, it was quantified neither by ITC nor by SPR.

**Anti-HIV-1 Activities of E2 GBV-C Peptides.** The antiviral activity of E2 GBV-C synthetic peptides was analyzed by means of three complementary assays. We first examined the effect of E2 peptides on cell–cell fusion assays, analyzing their capacity to block syncytium formation between HeLa cells expressing the envelope protein of HIV-1 and TZM-bl cells expressing the human CD4 receptor CXCR4 or CCR5 HIV-1 co-receptors in the presence of various amounts of each peptide.

The half maximal inhibitory concentration ( $\text{IC}_{50}$ ) as a measure of the effectiveness of each E2 peptide in inhibiting

**Table 2.** Kinetics Parameters of the Interaction between the E2 GBV-C Peptides and HIV-1 FP Determined Using ITC and SPR

peptide	ITC		SPR		
	$K_A$ ( $\text{M}^{-1}$ )	$K_D$ (M)	$K_a$ ( $\text{M}^{-1} \text{s}^{-1}$ )	$K_d$ ( $\text{s}^{-1}$ )	$K_D$ (M)
P11	$(3.00 \pm 0.58) \times 10^4$	$3.33 \times 10^{-5}$	$(0.23 \pm 0.005) \times 10^3$	$(5.8 \pm 0.13) \times 10^{-3}$	$2.52 \times 10^{-5}$
P45	$(1.57 \pm 1.05) \times 10^4$	$6.36 \times 10^{-5}$	$(0.13 \pm 0.005) \times 10^3$	$(7.74 \pm 0.34) \times 10^{-3}$	$5.86 \times 10^{-5}$
P59	ND	ND	ND	ND	ND
P97	$(2.52 \pm 1.16) \times 10^5$	$3.96 \times 10^{-6}$	$(1.28 \pm 0.004) \times 10^4$	$(2.86 \pm 0.23) \times 10^{-3}$	$2.24 \times 10^{-6}$
P105	$(5.00 \pm 0.73) \times 10^4$	$2.00 \times 10^{-5}$	$(0.41 \pm 0.008) \times 10^3$	$(7.17 \pm 0.14) \times 10^{-3}$	$1.76 \times 10^{-5}$

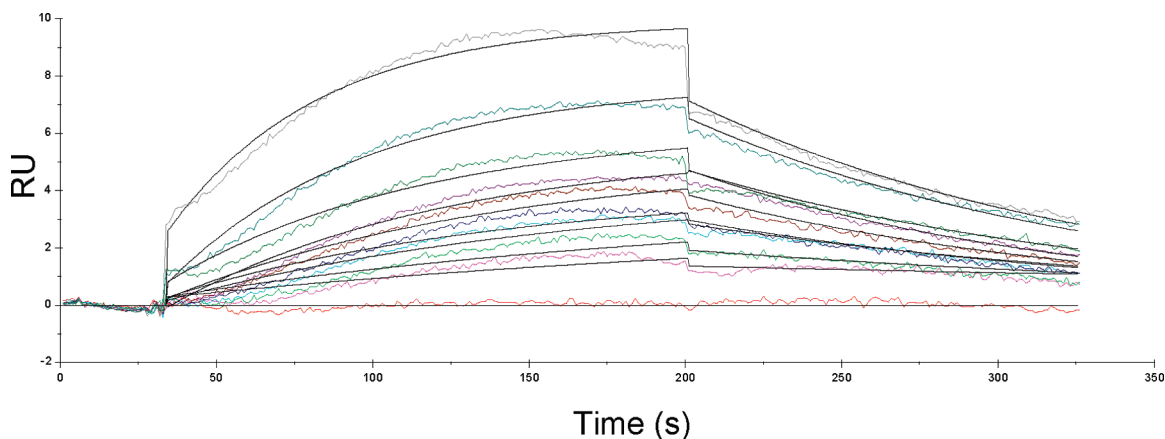


**Figure 5.** Sensorgrams for the direct binding of P105 to immobilized HIV-1 FP. P105 concentrations ranged from 0 to 100  $\mu\text{M}$ . Black lines are fits to a 1:1 Langmuir binding model.

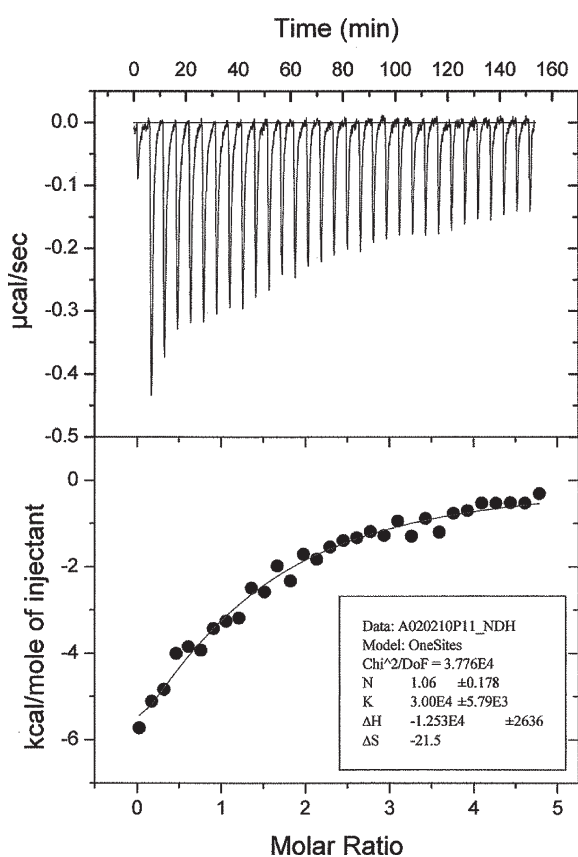


**Figure 6.** Calorimetric titration of HIV-1 FP with the P11 GBV-C peptide at 25 °C.

syncytium formation is shown in Table 3. The following 18-mer peptides P11, P19–21, P23, P25, P45–47, P59, P97, P109, and P124 inhibited the gp41-induced cell–cell fusion in a dose-dependent manner, showing  $\text{IC}_{50}$  values between 141.2 and 832.9  $\mu\text{M}$  (Figure 2 in Supporting Information). The remaining peptides showed less than 50% of inhibition or had a non-sigmoidal (neither linear) shape of the dose-response curve, and they were discarded. C34 peptide was used as positive control ( $\text{IC}_{50} = 0.023 \mu\text{M}$ ; 95% CI = 0.021–0.025). As an example, in Figures 7 and 8 we show how P45 inhibits syncytium formation in a dose-dependent manner.

The preliminary analysis performed to assess the capability of the 124 E2-peptides to inhibit the HIV-1 infection of

CEM174 showed that all of them were able to inhibit the p24 antigen release at a high concentration of 500  $\mu\text{M}$ , but only a subset of them produced more than 50% HIV-1 inhibition at 250  $\mu\text{M}$  (P11, P19–P21, P23, P25, P34, P46, P47, P97, and P109) at day 7 postinfection (Figure 9).

These data were confirmed when the inhibitory effect of viral infection was analyzed using the TZM-bl cell line. Only the peptides P11, P19–P21, P34, P45–P47, P109, and P124 were able to inhibit the HIV-1 infection of HIV-1<sub>HXB2</sub> (R4), the primary isolate HIV-1<sub>69/7</sub> (R5X4 dual or mixed tropism (DM)), and HIV-1<sub>BaL</sub> (R5) in a dose-dependent manner (Figure 3 in Supporting Information). The inhibitory effect was differentially efficient between the X4 and the R5 strains. The  $\text{IC}_{50}$  obtained with peptides P11, P19, P20, and P21 for HIV-1<sub>HXB2</sub> was as follows: < HIV-1<sub>69/7</sub> < HIV-1<sub>BaL</sub>; nevertheless, the  $\text{IC}_{50}$  obtained with peptides P34, P45, P46, P47, and P109 for HIV-1<sub>69/7</sub> was < HIV-1<sub>HXB2</sub> < HIV-1<sub>BaL</sub>. In Figure 10 we show as an example the dose-response curves obtained for P47. In general, all peptides tested showed an  $\text{IC}_{50}$  that was 1 log higher for the virus X4 or R5X4 DM (Table 4). Of note was that the P124 was only effective for the HIV-1<sub>BaL</sub> strain.

With the aim of locating where the most active peptide fragments lie on the E2 protein, a computerized prediction analysis of hydrophilicity, accessibility, and presence of  $\beta$ -turns of the E2 protein according to Hopp and Woods,<sup>23</sup> Janin,<sup>24</sup> and Chou and Fasman<sup>25</sup> was performed. In general, it was observed that the selected peptide regions showed high indexes of hydrophilicity and accessibility and a large number of residues with high turn probability that tend to distribute on the surface of the protein. In Supporting Information (Figure 4) we have incorporated the profiles of the E2 protein as well as noted the selected peptide regions.

New experiments performed in TZM-bl on which the peptides were incubated with the cell for 2 h before the virus adsorption did not prevent the viral infection.

The inhibitory effect of peptides P11, P19–P21, P34, P45–P47, P109, and P124 to inhibit infection of peripheral blood mononuclear cells (PBMCs) was also observed. In this case, the qualitative analysis of p24 antigen produced in these cell cultures showed (1) that the concentrations up to which viral production was almost undetectable were lower than the  $\text{IC}_{50}$  observed in TZM-bl cell cultures, (2) that these concentrations were lower in HIV-1<sub>HXB2</sub> (R4) than HIV-1<sub>BaL</sub> (R5) with the exceptions of P19, P46, and P124, and (3)

**Table 3.** Inhibitory Activity of E2 Peptides on Gp41-Mediated Cell–Cell Fusion Assay

peptide	residue no. <sup>a</sup>	sequence	IC <sub>50</sub> <sup>b</sup> (μM)	95% CI <sup>c</sup>
P11	31–48	TGEKVWDRGNVTLLCDCP	439.7	361.4–535.0
P19	55–72	LPAFCQAIGWGDPIHWS	369.5	314.8–433.7
P20	58–75	FCQAIGWGDPIHWSHGQ	347.6	305.1–396.0
P21	61–78	AIGWGDPIHWSHGQNRW	832.9	754.5–919.4
P23	67–84	PITHWSHGQNRWPLSCPQ	508.8	496.9–520.9
P25	73–90	HGQNRWPLSCPQVYVGSV	304.4	260.9–355.3
P45	133–150	SDRDTVVELSEWGVPCAT	141.2	129.1–154.4
P46	136–153	DTVVELSEWGVPCATCIL	428.8	373.1–429.7
P47	139–156	VELSEWGVPCATCILDRR	330.8	277.4–394.5
P59	175–192	RFPFHRCGAGPKLTKDLE	529.6	514.0–545.8
P97	289–306	LVRRRSELMGRRNPVCPG	537.6	476.9–606.0
P109	325–342	LQEVDAAGNFIPPPRWLL	687.1	616.3–766.1
P124	370–387	WVNQLAVLGLPAVDAAVA	332.7	265.4–417.1

<sup>a</sup>The residue number of each region corresponds to its position in E2 (U45966\_usa) of GBV-C. <sup>b</sup>IC<sub>50</sub>: concentration of a peptide causing 50% inhibition of cell–cell fusion (μM). <sup>c</sup>95% CI: 95% confidence interval of IC<sub>50</sub>.

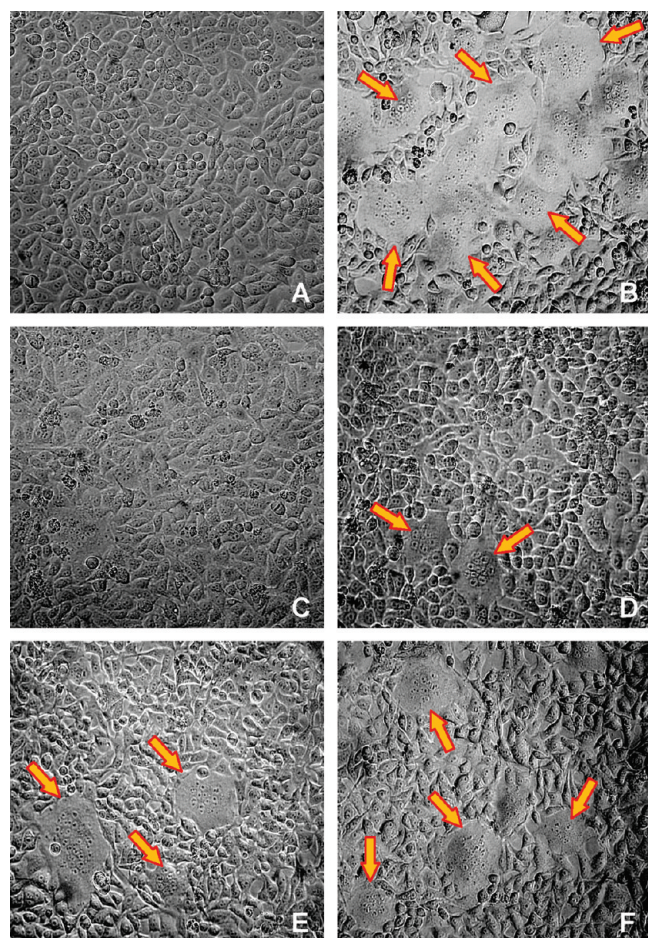


**Figure 7.** Inhibition of gp41-induced cell–cell fusion by incubation with P45 peptide. The arrow indicates syncytia (large cell-like structure filled with cytoplasm containing many nuclei) formation. Cells grown in 96-well plates were treated with C34 (1.2 μM) in (A) or with P45 peptide: (C) 500 μM, (D) 250 μM, (E) 125 μM, and (F) 62.5 μM. (B) corresponds to untreated control.

that the sets P19–P21, P45–P47, P109 were more efficient in inhibiting the HXB2 virus than P11 and P34 and that P124 is more efficient in regard to BAL (Table 5).

## Discussion

The understanding of how a nonpathogenic human virus, GBV-C, interferes with HIV related disease progression has

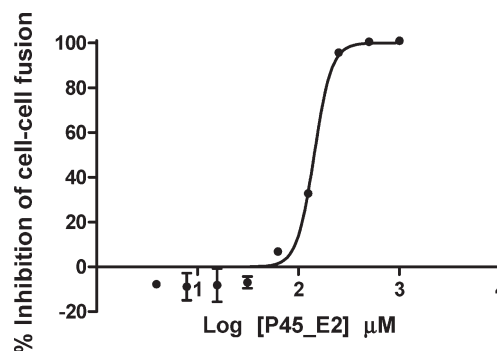


**Figure 8.** Inhibitory activity of P45 peptide of gp41-induced cell–cell fusion. Each data point represents the mean percent inhibition ± standard error (bars).

been studied in the past years by means of epidemiological studies of HIV-infected cohorts and by in vitro approaches related to GBV-C/HIV co-infection. It has been proposed that the GBV-C E2 protein may modify HIV disease progression. In addition the GBV-C E2 protein, when added to CD4<sup>+</sup> T cells, inhibits HIV entry in a HIV-1 pseudotyped retrovirus single infection system. Moreover, polyclonal anti-E2 antibodies and murine monoclonal anti-E2 antibodies neutralized a broad panel of HIV-1 isolates in vitro.

We here present data that peptides derived from the GBV-C E2 protein are able to reduce HIV-1 in vitro. We show that several regions of the GBV-C E2 represented by the following peptides (GBV-C E2<sub>31–48</sub>, P11; GBV-C E2<sub>55–78</sub>, P19–P21; GBV-C E2<sub>100–118</sub>, P34; GBV-C E2<sub>133–156</sub>, P45–P47; GBV-C E2<sub>289–306</sub>, P97; GBV-C E2<sub>325–342</sub>, P109; GBV-C E2<sub>370–387</sub>, P124) can be implicated in the inhibition of the HIV-1 at the entry level.

The observed inhibition events were probably mediated by blocking virus entry, as observed by the biophysical assays performed in the presence of the gp41 HIV-1 fusion peptide like the inhibition of vesicular contents induced by the HIV-1 FP or the binding to POPG vesicles. As described, we could determine by calorimetric and surface plasmon resonance techniques the interaction of several domains of GBV-C E2 protein and the HIV-1 FP. According to the ITC results, the binding of both peptides is characterized by negative enthalpies, suggesting that there are a large number of favorable hydrogen bond contacts or van der Waals interactions between the E2 peptides and HIV-1 FP. On the other hand, the unfavorable entropic change could indicate that the binding

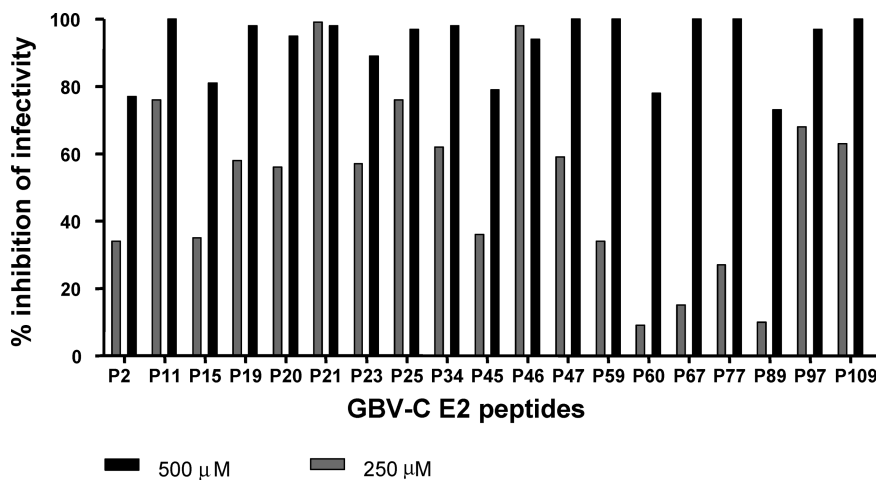


**Figure 9.** Inhibition of the HIV-1 infection of CEM174 by GBV-C E2 peptides.

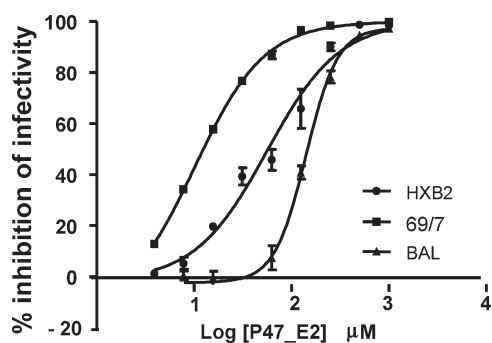


**Figure 10.** Susceptibilities of three different HIV-1 strains to P47 peptide in TZM-bl cells.

of E2 peptides to HIV-1 FP can be associated with structuring processes.<sup>26</sup>

The individual analysis of 124 overlapped GBV-C E2 peptides demonstrated that P11, P19–P21, P34, P45–P47, P109, and P124 inhibit the HIV-1 infection of X4, X4R5 DM, and/or R5 strains in a dose-dependent manner in TZM-bl cell cultures. Of note are that the potencies of E2 peptides to inhibit the HIV-1 viral infection are modest ( $IC_{50}$  values in the micromolar range), the concentration needed to inhibit the viral infection being higher compared to another entry inhibitor,<sup>27</sup> and that the sensitivity of HIV-1 to these peptides was apparently modulated by the viral tropism.

In relation to the concentration of peptides required, it was highly reduced when the susceptibility assays were performed by using PBMCs. The activity enhancement observed in PBMCs vs TZM-bl cell line could be explained by the influence of the density of receptors and co-receptors and viral replication capacity in each cell type, as well as the target cell environment in which the induction of soluble factor release could hinder HIV-1 entry, as has been described elsewhere.<sup>28–30</sup> In any case, new studies are being conducted to analyze the effects of these particular peptides on uninfected PBMCs, and the chemical modification of peptides will be carried out to reduce the  $IC_{50}$ s observed.

In a comparison of the inhibitory activity of GBV-C E2 peptides on gp41-mediated cell–cell fusion and the susceptibility of HIV-1 to them, we consider the relevance mainly of domains GBV-C E2<sub>55–78</sub> and E2<sub>133–156</sub> in terms of future drug design. These domains might comprise useful leads for optimization because of the many advantages that peptides

bring to the clinic, like potency, specificity, and lower rates of toxicity.

On the basis of the peptide sequences selected, the design and synthesis of new forms of peptide presentation are considered in order to enhance the antiviral activity of these synthetic molecules. The literature has described different strategies to increase the antiviral activity of synthetic peptides that prevent the limitations presented by this type of molecule in its clinical application, such as reduced stability and limited selectivity of action. Hence, the introduction of non-natural residues, such as D-amino acids, has recently been described to avoid peptide degradation by proteases or the introduction of intramolecular cyclical motives to encourage a more rigid structure with less flexibility in them.<sup>19</sup> Another recent approach consists of a modification of peptides by combining them with fatty acids, which favors enzymatic stability, improves pharmacokinetic properties, and encourages secondary structure in the synthetic peptide sequence. The modification of peptides that inhibit HIV fusion through the combination of fatty acids to increase their inhibiting activity has recently been described.<sup>31</sup> This inhibiting activity is correlated to the length of the fatty acid, the direction of the fatty acid attachment (N- or C-terminal) to the peptide sequence, and the peptide concentration in cells. It seems that the fatty acid allows the combined peptide to become attached to the cell membrane surface, increasing the concentration of the combined peptide at points of fusion.

In relation to the viral tropism, in general, the  $IC_{50}$  values observed for the HIV-1<sub>HXB2</sub> (X4) were lower than those for HIV-1<sub>69/7</sub> (R5X4 DM) and lower than those for HIV-1<sub>BaL</sub> (R5), reaching 1  $\log_{10}$  difference between the X4 strain and the R5 strain. This sensitivity profile was also observed in the PBMC susceptibility assays performed. The incubation of peptides and TZM-bl before the HIV-1 adsorption did not prevent the viral infection of either HIV-1<sub>HXB2</sub> or HIV-1<sub>BaL</sub> laboratory adapted strains. Thus, we discard that peptide–co-receptor binding as the cause of the differential susceptibility between both viral strains.

A similar phenomenon was observed in the T-20-gp41 interaction by Derdeyn et al.<sup>32,33</sup> in which the  $IC_{50}$  obtained for R5 isolates was 0.8  $\log_{10}$  higher than the mean  $IC_{50}$  for X4 isolates. This feature was interpreted as a consequence of the differential affinities of proteins during the cooperative process of CD4-gp120-CCR5 binding and the CD4-gp120-CXCR4 binding, leading to conformational changes that

**Table 4.** Phenotypic Susceptibilities of HIV-1 to E2 GBV-C Peptides in TZM-bl Cells

peptide	HXB2		BAL		69-7 <sup>a</sup>	
	IC <sub>50</sub> <sup>b</sup>	95% CI <sup>c</sup>	IC <sub>50</sub> <sup>b</sup>	95% CI <sup>c</sup>	IC <sub>50</sub> <sup>b</sup>	95% CI <sup>c</sup>
P11	162.1 <sup>d</sup>	125.3–209.7	484.5	441.6–531.5	208.8	178.8–243.9
P19	46.0	34.5–61.2	194.3	171.2–220.5	71.4	64.7–78.7
P20	70.1	60.5–81.2	125.5	124.4–126.7	111.1 <sup>d</sup>	104.8–117.7
P21	44.9	36.8–54.7	529.1	427.3–655.2	371.1 <sup>d</sup>	326.4–421.9
P34	237.4	191.3–294.6	411.2	373.5–452.7	118.6	111.6–126.0
P45	48.8 <sup>d</sup>	42.3–56.2	505.5	501.3–509.8	43.7	38.4–49.7
P46	39.9 <sup>d</sup>	34.7–45.8	462.8	438.7–488.2	24.1	22.0–26.5
P47	58.6 <sup>d</sup>	50.6–67.8	140.3	125.9–156.4	20.1	18.1–22.2
P109	37.5	31.8–44.3	294.8 <sup>d</sup>	259.2–335.3	60.8	55.1–67.1
P124			94.7	79.9–112.3		
C34	nd <sup>e</sup>	nd <sup>e</sup>	0.012	0.010–0.013	nd <sup>e</sup>	nd <sup>e</sup>
T20	nd <sup>e</sup>	nd <sup>e</sup>	0.021	0.019–0.022	nd <sup>e</sup>	nd <sup>e</sup>
amphotericin B	0.175	0.167–0.185	0.136	0.129–0.145	nd <sup>e</sup>	nd <sup>e</sup>

<sup>a</sup>One replicate for each peptide in this assay. <sup>b</sup>IC<sub>50</sub>: concentration ( $\mu$ M) of a peptide causing 50% inhibition of the infection, obtained from two independent experiments. <sup>c</sup>95% CI: 95% confidence interval of IC<sub>50</sub>. <sup>d</sup>Linear mathematical model, not sigmoidal. <sup>e</sup>nd: not determined.

**Table 5.** Concentrations of E2 Peptides ( $\mu$ M) up to Which the HIV-1 Infection of PBMCs Was Not Detected at Day 7 of Cell Culture by Qualitative Analysis of p24 Antigen

	HXB2	BAL
P11	31.2	62.5
P19	15.6	15.6
P20	7.8	15.6
P21	3.9	62.5
P34	31.2	62.5
P45	7.8	31.2
P46	7.8	7.8
P47	7.8	15.6
P109	7.8	15.6
P124	62.5	7.8

promote T-20 interaction with HR1 binding when the virus uses the CXCR4 co-receptor during virus-cell fusion. In our study, we do not discard the notion that the gp120-CXCR4 binding could also promote the display of gp41-FP binding sites for the active GBV-C E2 peptides. On the other hand, despite the FP having a highly preserved 23 amino acid sequence among the HIV-1 strains, the polymorphism L/V was observed in the seventh position of the N-terminal FP of gp41 of the HIV-1<sub>BaL</sub> laboratory adapted strain. This polymorphism located in the  $\alpha$ -helix conformation of FP<sup>34</sup> did not appear as a consequence of an adaptive viral escape in the presence of peptides; however, its presence could be the cause of the differential affinity to the peptides observed between both laboratory adapted viral strains, independent of viral tropism. Future studies with the improved peptides will be carried out to assess this hypothesis.

To sum up, in the present article we describe certain E2 GBV-C domains that interfere with the HIV-1 fusion peptide-vesicle interaction, produce a notable decrease the cellular membrane fusion, and interfere with the HIV-1 infectivity in a dose-dependent manner. We provide insights into GBV-C E2 driven inhibition of HIV-1 replication that may lead to the identification of novel therapeutics, drug targets, and putative candidate vaccine antigens.

## Experimental Section

**Peptide Synthesis.** The 124 peptides of the E2 GBV-C envelope protein were synthesized by semiautomated multiple solid-phase peptide synthesis on a peptide synthesizer (SAM, Multisynth, Germany) as C-terminal carboxamides on a Tentagel RAM resin (Rapp Polymere GmbH, Germany) (100 mg, 0.2 meq/g)

and following a 9-fluorenylmethoxycarbonyl (Fmoc) strategy. Amino acid side chain protection was effected by the following: triphenylmethyl (Trt) for glutamine, asparagine, histidine, and cysteine; *tert*-butyl (<sup>t</sup>Bu) for aspartic acid, glutamic acid, serine, threonine, and tyrosine; 2,2,5,7,8-pentamethylchroman-6-sulfonyl (Pmc) for arginine, and *tert*-butoxycarbonyl (Boc) for lysine and tryptophan.

The coupling reaction was performed using 4-fold molar excesses of activated Fmoc-amino acids throughout the synthesis. The amino acids were activated essentially by means of treatment with 2-(1*H*-7-azabenzotriazole-1-yl)-1,1,3,3-tetramethyluranyl hexafluorophosphate methanaminium (HATU) and a base such as diisopropylethylamine (DIPEA). The Fmoc-deprotection step was accomplished twice with 20% piperidine in dimethylformamide (DMF) for 10 min. The efficiency of these reactions was evaluated by the ninhydrin colorimetric reaction.

Once the synthesis was complete, the cleavage and deprotection processes of the peptidyl resins were carried out in a semiautomated synthesizer using the Multisynth accessories available for this purpose. These reactions took place by means of treatment with 94% trifluoroacetic acid (TFA) in the presence of scavengers, basically 2.5% H<sub>2</sub>O, 2.5% 1,2-ethanedithiol (EDT), and 1% triisopropylsilane (TIS) for 4 h.

Peptides were isolated by precipitation with cold diethyl ether, centrifuged, and lyophilized in 10% acetic acid. The peptides were characterized by analytical HPLC on a Kromasil C-18 column (Teknokroma, 5  $\mu$ m, 25 cm  $\times$  0.46 cm) with a linear gradient of 95–5% A in B over 20 min at a flow rate of 1 mL/min using 0.05% TFA in water (A) and 0.05% TFA in acetonitrile (B) as the eluting system. The peptides were up to 90% pure by analytical HPLC at 215 nm. Their identity was confirmed by electrospray mass spectrometry (ES-MS) (Table 1 in Supporting Information). Crude peptides were desalted using Oasis HLB Plus cartridge 225 mg/60  $\mu$ g from Waters. These cartridges contain a polymeric water-wettable reversed phase sorbent.

The highly preserved gp41 FP, AVGIGALFLGFLGAAGS-TMGAAS, was successfully synthesized in a 100% polyethylene glycol based resin, the ChemMatrix, that has proved to be a superior support for the solid-phase synthesis of hydrophobic and highly structured peptides.<sup>35,36</sup> Peptides synthesized manually (P2, P11, P19–21, P23, P25, P34, P45–47, P59, P97, P105, P109, P124, and FP gp41) were purified by preparative HPLC in a Kromasil-C8 column (Teknochroma, 5  $\mu$ m, 25 cm  $\times$  2.2 cm) and characterized by ES-MS. The purity by HPLC of all peptides was  $\geq$ 95%.

**Inhibition of the Release of Vesicular Contents Induced by the HIV-1 FP.** In order to select the E2 GBV-C peptide sequences that have the capacity to inhibit the interaction and destabilization process of membranes induced by the HIV-1 fusion peptide,

the biophysical assay on the vesicle contents release described by Ellens<sup>37</sup> was performed in a PTI QM4CW spectrofluorimeter (Photon Technology Internacional). Unilamellar lipid vesicles (LUVs) containing fluorescent probes ANTS and DPX were prepared according to the protocol described by our work group.<sup>38</sup>

In order to carry out screening of the synthesized peptides, the concentration of the gp41(1–23) fusion peptide (HIV-1 FP) providing approximately half the total vesicle contents release was selected. Each GBV-C peptide sequence corresponding to the E2 protein was premixed with the HIV-1 FP in DMSO prior to its addition to a suspension of LUV liposomes. Dequenching of coencapsulated ANTS and DPX fluorescence resulting from dilution was measured to assess the leakage of aqueous contents from vesicles.

ANTS/DPX leakage out of the LUVs (100  $\mu$ M lipids) was measured after 30 min of incubation at room temperature. Leakage was monitored by measuring the increase in ANTS/DPX fluorescence intensity at 520 nm, with an excitation of 355 nm. HIV-1 FP/E2 peptide ratios ranged from  $1/1$  to  $1/10$ . The percentage of leakage was calculated as

$$\% \text{ leakage} = [(F - F_0)/(F_{100} - F_0)] \times 100$$

where  $F_0$  is the initial fluorescence of LUVs,  $F$  is the fluorescence intensity after incubation with the peptide, and  $F_{100}$  is the fluorescence intensity after addition of 10  $\mu$ L of a 10% (v/v) Triton-100 solution (complete lysis of the LUV).

**Effect of E2 Peptides on the HIV-1 FP Binding to Model Membranes.** POPG LUVs were prepared according to the protocol described by Rojo et al.<sup>39</sup> Emission fluorescence spectra were recorded for peptides in tris(hydroxymethyl)aminomethane (Tris), 10 mM, pH 7.4, at 20 °C. Peptide–phospholipid interactions were assessed by monitoring the changes in the fluorescence spectra when LUV-POPG liposomes were incubated with 2  $\mu$ M HIV-1 FP. Moreover, each E2 peptide (P59, P97, and P105) was premixed (1:1 ratio) with the HIV-1 FP in dimethyl sulfoxide (DMSO) prior to its titration with POPG liposomes. Regarding the presence of a Trp residue in both P11 and P45 sequences, these E2 peptides were not evaluated in this assay.

The fluorescence intensity was measured as a function of the lipid/peptide ratio. Suspensions were continuously stirred and were left to equilibrate for 1 min before recording the spectrum. Fluorescence intensities were corrected for contribution of light scattering by subtraction of the appropriate vesicle blank. The last correction was obtained from a parallel lipid titration of *N*-acetyltryptophanamide (NATA), which is known to not interact with lipids.

According to Wimley and White<sup>40</sup> and assuming a two-state equilibrium between water-soluble aggregates and membrane-bound peptides, the apparent mole fraction partition coefficients were determined by fitting the binding curves to the equation  $I = f_{\text{bound}}I_{\text{max}} + (1 - f_{\text{bound}})I_0$ , for which  $I$  is the relative fluorescence intensity,  $I_0$  is the intensity in the absence of lipid, and  $f_{\text{bound}} = K_x L / (W + K_x L)$ , where  $K_x$  is the mole fraction partition coefficient,  $L$  is the lipid concentration, and  $W$  is the molar concentration of water (55.3 M at 25 °C).

**Surface Plasmon Resonance Studies.** Surface plasmon resonance (SPR) studies were performed on a Biacore T100 instrument (GE, Healthcare). The surface of a CM5 chip with a dextrane matrix was activated by injecting a mixture of *N*-hydroxysuccinimide (NHS) and *N*-ethyl-*N'*-(dimethylaminopropyl)carbodiimide (EDC) for 7 min at a low rate of 10 mL/min. The HIV-1 FP was dissolved in sodium acetate buffer, pH 4.5, and the dissolution was filtered and injected onto the activated surface of the sensor chip until the immobilization level of 100–500 RU was reached. The surface was capped with a 1 M solution of ethanolamine at pH 8.0 to remove residual activated carboxylic acid functional groups. Control experiments were performed using sensor chips activated according to the protocol described but without any peptide

coupled. The analytes (E2 peptides) were dissolved in HBS buffer (10 mM HEPES, pH 7.4, 150 mM NaCl, 3.4 mM EDTA, 0.05% surfactant P20) and injected onto the surface of the sensor chip diluted in a range of concentrations between 1.5 and 100  $\mu$ M at a flow rate of 15 mL/min. The association and dissociation times were 180 s each. Regeneration was performed using a 50 mM NaOH and 1 M NaCl solution. The interaction parameters were analyzed and evaluated using the Biacore T100 GxP Evaluation software.

**Isothermal Titration Calorimetry Studies.** Isothermal titration calorimetric (ITC) experiments were recorded on VP-ITC microcalorimeter (MicroCal, LLC, Northampton, MA). Purified peptides were dissolved in DMSO and then degassed for 5 min prior to sample loading. Briefly, a solution of 0.5 mM peptides in DMSO was injected into a chamber containing 25  $\mu$ M HIV-1 FP. The calorimeter was first equilibrated at 20 °C, and the baseline was monitored during equilibration. The time between injections was 5 min, and the stirring speed was 300 rpm. The heats of dilution were determined in control experiments by injecting E2 peptides into DMSO and subtracting from the heats produced in the corresponding peptide–peptide binding experiments. Control experiments were also performed by titrating DMSO into HIV-1 FP. The total observed heat effects were corrected for these small contributions. All titration data were subsequently analyzed using the Origin 7 software (MicroCal, LLC).

**Inhibition of Cell Binding.** Two cell lines were used: HeLa-env (donated by Dr. Blanco from Fundació IRSI Caixa) expressing the protein from the HIV-1 envelope and including the HIV-1 long terminal repeat (LTR) promoter in its genome, and TZM-bl (AIDS reagents catalogue no. 8129), which expresses the membrane receptor from CD4 lymphocytes and co-receptors CCR5 and CXCR4 and includes the luciferase and  $\beta$ -galactosidase genes in its genome.<sup>41–43</sup>

Cell lines were cultured in Dulbecco's modified Eagle medium (DMEM, PAA) containing L-glutamine and sodium pyruvate supplemented with 10% heat-inactivated fetal bovine serum (FBS), 100  $\mu$ g/mL penicillin, and 100  $\mu$ g/mL streptomycin. The cell cultures were maintained in a tissue culture incubator at 37 °C in a 5% of CO<sub>2</sub> atmosphere.

When both types of cells are cocultured, cell membrane fusion occurs and the luciferase is activated and produced the oxidation of luciferine. The level of oxiluciferine was quantified by using the Britelite kit (Perkin-Elmer) and SpectraMax M5 microplate reader.

In this study, the trial on the inhibition of cell binding induced by E2 GBV-C peptides consisted of the incubation of 2500 HeLa-env cells/well (Nunc plates, catalogue no. 136101) for 1 h at serial dilutions (5–1000  $\mu$ M) of the peptides to be tested, followed by the addition of around 10 times (25 000 cells) TZM-bl/well and incubation for 24 h.

To control cell binding, wells without peptides were reserved and a known cell binding inhibitor, C-34 (AIDS Reagents, catalogue no. 9824), was used as a positive control.

The level of inhibition of cell binding was also qualitatively assessed by observing the formation of syncytia under the microscope.

**Inhibition of HIV-1 Infection. Preliminary Screening of Peptides Inhibitory Effect on HIV-1.** A preliminary susceptibility assay of HIV-1 against the 124 E2 GBV-C peptides was performed by infecting CEM-174 cell line (AIDS Reagents, catalogue no. 272) with 0.008 multiplicity of infection (moi) of HIV-1<sub>92UG024</sub> (R4 tropism, subtype D, AIDS Reagents no. 1649) and two different concentrations of each peptide (500 and 250  $\mu$ M). Briefly, the 600 TCID<sub>50</sub> (50% tissue culture infective dose) of virus was first incubated, in triplicate with each concentration of each peptide prepared on RPMI-1640 cell medium supplemented with 10% of fetal bovine serum (FBS), for 2 h at 37 °C and 5% of CO<sub>2</sub>. The peptide C34 (AIDS Reagents, no. 9824) at 1  $\mu$ M was used as inhibition control. Later, 75 000 cells were added



and incubated for an additional 2 h at 37 °C and 5% of CO<sub>2</sub>. After viral adsorption, the infected cells were washed three times with phosphate buffered saline (PBS) and incubated for 7 days in the presence of each concentration of each peptide in a final volume of 200 μL/well in 96-well tissue culture plates. Triplicates of infected cells without peptide and noninfected cells were included as positive and negative controls of infection, respectively. Viral infection was analyzed by cytopathic effect and by ELISA HIV-1 p24 ELISA p24 antigen-HIV-1 (Ag HIV, Innogenetics no. K1048).

**Susceptibility Assay on TZM-bl.** A set of peptides with potential capability for HIV-1 inhibition demonstrated by biophysical assays, cell–cell fusion assays, and preliminary assays on HIV-1 susceptibility in CEM 174 assay were investigated more deeply in a susceptibility assay on TZM-bl cells to assess if the inhibition of HIV-1 infection was in a dose-dependent manner.

Briefly, triplicates of 2-fold serial concentration of each peptide (0–500 μM) were preincubated along with a predetermined volume of either HIV-1<sub>BaL</sub> strain (R5 tropism, AIDS Reagent) or HIV-1<sub>HXB2</sub> strain (R4 tropism, obtained from pHXB2, kindly provided by Prof. C Boucher, University of Utrecht (AZU), The Netherlands) or a HIV-1 primary isolate named 69/7 (R5X4 dual or mixed tropism DM, isolated from an infected patient), in a final volume of 100 μL/well of DMEM with 10% FBS in 96-cell culture plates, for 2 h at 37 °C and 5% of CO<sub>2</sub>. In addition, 2-fold serial concentration of either T-20 (AIDS Reagents, no. 9409) or C34 or amphotericin B (Bristol-Myers Squibb, SL) was used as a dose-dependent inhibition control of the assay. Later, an amount of 100 μL of cell media containing 15 000 TZM-bl cells was added to each well. In these conditions the final moi of each viral strain was 0.02 HIV-1<sub>BaL</sub> and 0.01 for HIV-1<sub>HXB2</sub> and HIV-1<sub>69/7</sub>, respectively. A triplicate of each HIV-1 infected TZM-bl without peptides and a triplicate of noninfected cells were used as positive and negative controls, respectively, and they were included in each assay. After 72 h postinfection, the supernatant of each well was removed and to it was added 50 μL of lysis buffer (0.1% TritonX-100, 10 mM MgCl<sub>2</sub>, 0.5 mM dithiothreitol (DTT) in PBS) along with 50 μL of 1.5 mM of chlorophenolred-β-D-galactopyranoside (CPRG). The β-galactosidase activity was analyzed by spectrophotometry (570 nm, SpectraMax M5 microplate reader). The optical densities obtained were transformed in percentage of inhibition, and the sigmoid curves were analyzed by nonlinear regression (GraphPad Prism software, version 5). In parallel, the toxicity effect on TZM-bl cells at each concentration of peptide assayed was analyzed by using the 3-(4,5-dimethylthiazol-2-yl)-2,5-diphenyltetrazolium bromide (MTT) assay as it is described below.

A modification of this procedure was also tested to determine if the inhibitory effect of the peptides was due to a direct interaction with the receptor or co-receptor of viral entry. In this case, the TZM-bl cells were incubated with the 2-fold serial concentrations of peptides for 2 h at 37 °C and 5% of CO<sub>2</sub> and washed three times with PBS prior to the viral adsorption period of 2 h. Later the cells were washed three times with PBS, incubated for 72 h in the absence of peptides, and analyzed as described above.

**Susceptibility Assay on PBMCs.** A qualitative assay of HIV-1 susceptibility based on the p24 HIV-1 antigen was performed by infecting PBMCs with HIV-1<sub>HXB2</sub> and HIV-1<sub>BaL</sub> to corroborate the peptide's inhibitory effect of HIV-1 infection of this type of cell. The PBMCs were obtained from healthy donor buffy coats by density gradient centrifugation (ACCUSPIN System-Histopaque-1077, Sigma Diagnostics) and activated with 5 μg/mL of phytohemagglutinine (PHA, Sigma-Aldrich) in RPMI-1640 media (Lonza-BioWithaker) and 10% of FBS for 24–72 h prior the viral infection. The 2-fold serial concentrations of peptides (0–125 μM) were prepared in RPMI-1640 supplemented with 10% of FBS and 10 U/mL recombinant interleukine-2 (rIL-2, Roche Diagnostic Systems) and preincubated along with a

predetermined volume of either HIV-1<sub>HXB2</sub> or HIV-1<sub>BaL</sub> for 2 h at 37 °C and 5% of CO<sub>2</sub>. Later, 8 × 10<sup>5</sup> activated PBMCs were added and incubated for an additional 2 h to allow viral adsorption. Finally the infected cells were washed three times with PBS and incubated for 7 days, along with their corresponding concentrations of peptide, in 96-well cell culture plates containing 200 × 10<sup>3</sup> PBMC in 200 μL of RPMI-1640, 20% of FBS, and 10 U/mL of rIL-2 in the absence of peptides. Thus, the final moi for each viral strain was 0.001. Viral release was analyzed by qualitative ELISA p24 antigen-HIV-1 (Ag HIV, Innogenetics, no. K1048).

**Cell Viability with MTT Assay.** Cell toxicity of E2 peptides was analyzed in HeLa, TZM-bl, and PBMCs using the MTT assay. Cells were cultured with DMEM (15 000 cells/well) in a 96-well plate and incubated with the serial dilutions of each peptide at 37 °C for 72 h. Afterward, MTT was added to a final concentration of 7.5 mg/mL and incubated for 2 h at 37 °C. Later the medium was removed and 100 μL of DMSO was added to dissolve the formazan precipitate. Absorbance was measured at 570 nm after 45 min. Cell viability was determined by the quotient between the absorbance value of cells treated with peptide and untreated cells. The cytotoxic concentration (CC<sub>50</sub>) was analyzed by nonlinear regression.

**Statistical Analysis.** To estimate the inhibitory concentration (IC<sub>50</sub>) of E2 peptides and its 95% confidence intervals, nonlinear regression models were used assuming a symmetrical sigmoidal four-parameters curve<sup>44</sup> for the relationship (GraphPad Prism 5.0 software). This parametrization of the sigmoidal curve has good statistical properties.

The response was used in the log form (log<sub>10</sub>(dose)) rather than the dose itself. After convergence of the models, goodness-of-fit was checked by looking to the replicates test, the residuals, the covariance matrix of the estimated parameters, the dependence of each estimated parameter, and the determination coefficient (R<sup>2</sup>). Constraints were used when necessary to improve the fit of the model.

**Acknowledgment.** This work was funded by Grants CTQ2006-15396-CO2-01/BQU and CTQ2009-13969-CO2-01/BQU from the Ministerio de Ciencia e Innovación, Spain. E.H. is the recipient of predoctoral grant (JAE program, CSIC, Spain). We also acknowledge Dr. Rafael Prohens (Scientific Parc of Barcelona), Dr. Ricardo Gutierrez (Pompeu Fabra University), and Dr. Julià Blanco (Fundació IRSI Caixa) for the discussion of ITC, SPR, and inhibition of cell–cell binding studies, respectively. The following reagent was obtained through the NIH AIDS Research and Reference Reagent Program, Division of AIDS, NIAID, NIH: HIV-1 IIIB C34 peptide from DAIDS, NIAID.

**Supporting Information Available:** Characterization of E2 GBV-C peptides; partitioning curves of FP and equimolecular mixtures of FP/E2 peptides (P59, P97, P105) in POPG LUVs; dose-response curves of inhibition of E2 GBV-C peptides for gp41-induced cell–cell fusion; dose-response curves of inhibition of E2 GBV-C peptides for HIV-1<sub>HXB2</sub>, HIV-1<sub>BaL</sub>, and primary isolate HIV-1<sub>69/7</sub> infection of TZM-bl cells; computerized prediction analysis of hydrophilicity, accessibility, and presence of β-turns in E2 protein. This material is available free of charge via the Internet at <http://pubs.acs.org>.

## References

- (1) Simons, J. N.; Leary, T. P.; Dawson, G. J.; Pilotmatias, T. J.; Muerhoff, A. S.; Schlauder, G. G.; Desai, S. M.; Mushahwar, I. K. Isolation of novel virus-like sequences associated with human hepatitis. *Nat. Med.* **1995**, *1*, 564–569.
- (2) Linnen, J.; Wages, J., Jr.; Zhang-Keck, Z. Y.; Fry, K. E.; Krawczynski, K. Z.; Alter, H.; Koonin, E.; Gallagher, M.; Alter, M.; Hadziyannis, S.; Karayiannis, P.; Fung, K.; Nakatsuji, Y.; Shih, J. W.; Young, L.;

- Piatak, M., Jr.; Hoover, C.; Fernandez, J.; Chen, S.; Zou, J. C.; Morris, T.; Hyams, K. C.; Ismay, S.; Lifson, J. D.; Hess, G.; Fong, S. K.; Thomas, H.; Bradley, D.; Margolis, H.; Kim, J. P. Molecular cloning and disease association of hepatitis G virus: a transfusion-transmissible agent. *Science* **1996**, *271*, 505–508.
- (3) Mphahlele, M. J.; Lau, G. K.; Carman, W. F. HGV: the identification, biology and prevalence of an orphan virus. *Liver* **1998**, *18*, 143–55.
- (4) Theodore, D.; Lemon, S. M. GB virus C, hepatitis G virus, or human orphan flavivirus? *Hepatology* **1997**, *25*, 1285–1286.
- (5) Heringlake, S.; Ockenga, J.; Tillmann, H. L.; Trautwein, C.; Meissner, D.; Stoll, M.; Hunt, J.; Jou, C.; Solomon, N.; Schmidt, R. E.; Manns, M. P. GB virus C/hepatitis G virus infection: a favorable prognostic factor in human immunodeficiency virus-infected patients? *J. Infect. Dis.* **1998**, *177*, 1723–1726.
- (6) Tillmann, H. L.; Heiken, H.; Knapik-Botor, A.; Heringlake, S.; Ockenga, J.; Wilber, J. C.; Goergen, B.; Detmer, J.; McMorris, M.; Stoll, M.; Schmidt, R. E.; Manns, M. P. Infection with GB virus C and reduced mortality among HIV-infected patients. *N. Engl. J. Med.* **2001**, *345*, 715–724.
- (7) Xiang, J.; Wunschmann, S.; Diekema, D. J.; Klinzman, D.; Patrick, K. D.; George, S. L.; Stapleton, J. T. Effect of coinfection with GB virus C on survival among patients with HIV infection. *N. Engl. J. Med.* **2001**, *345*, 707–714.
- (8) Zhang, W.; Chaloner, K.; Tillmann, H. L.; Williams, C. F.; Stapleton, J. T. Effect of early and late GB virus C viraemia on survival of HIV-infected individuals: a meta-analysis. *HIV Med.* **2006**, *7*, 173–180.
- (9) Van der Bij, A. K.; Kloosterboer, N.; Prins, M.; Boeser-Nunnink, B.; Geskus, R. B.; Lange, J. M.; Coutinho, R. A.; Schuitemaker, H. GB virus C coinfection and HIV-1 disease progression: The Amsterdam Cohort Study. *J. Infect. Dis.* **2005**, *191*, 678–685.
- (10) Williams, C. F.; Klinzman, D.; Yamashita, T. E.; Xiang, J.; Polgreen, P. M.; Rinaldo, C.; Liu, C.; Phair, J.; Margolick, J. B.; Zdonek, D.; Hess, G.; Stapleton, J. T. Persistent GB virus C infection and survival in HIV-infected men. *N. Engl. J. Med.* **2004**, *350*, 981–990.
- (11) Xiang, J.; George, S. L.; Wunschmann, S.; Chang, Q.; Klinzman, D.; Stapleton, J. T. Inhibition of HIV-1 replication by GB virus C infection through increases in RANTES, MIP-1alpha, MIP-1beta, and SDF-1. *Lancet* **2004**, *363*, 2040–2046.
- (12) Jung, S.; Knauer, O.; Donhauser, N.; Eichenmuller, M.; Helm, M.; Fleckenstein, B.; Reil, H. Inhibition of HIV strains by GB virus C in cell culture can be mediated by CD4 and CD8 T-lymphocyte derived soluble factors. *AIDS* **2005**, *19*, 1267–1272.
- (13) Moenkemeyer, M.; Schmidt, R. E.; Wedemeyer, H.; Tillmann, H. L.; Heiken, H. GBV-C coinfection is negatively correlated to Fas expression and Fas-mediated apoptosis in HIV-1 infected patients. *J. Med. Virol.* **2008**, *80*, 1933–1940.
- (14) Jung, S.; Eichenmuller, M.; Donhauser, N.; Neipel, F.; Engel, A. M.; Hess, G.; Fleckenstein, B.; Reil, H. HIV entry inhibition by the envelope 2 glycoprotein of GB virus C. *AIDS* **2007**, *21*, 645–647.
- (15) Xiang, J.; McLinden, J. H.; Chang, Q.; Kaufman, T. M.; Stapleton, J. T. An 85-aa segment of the GB virus type C NS5A phosphoprotein inhibits HIV-1 replication in CD4+ Jurkat T cells. *Proc. Natl. Acad. Sci. U.S.A.* **2006**, *103*, 15570–15575.
- (16) Chang, Q.; McLinden, J. H.; Stapleton, J. T.; Sathar, M. A.; Xiang, J. Expression of GB virus C NS5A protein from genotypes 1, 2, 3 and 5 and a 30 aa NS5A fragment inhibit human immunodeficiency virus type 1 replication in a CD4+ T-lymphocyte cell line. *J. Gen. Virol.* **2007**, *88*, 3341–3346.
- (17) Xiang, J.; McLinden, J. H.; Chang, Q.; Jordan, E. L.; Stapleton, J. T. Characterization of a peptide domain within the GB virus C NS5A phosphoprotein that inhibits HIV replication. *PLoS One* **2008**, *3*, No. e2580.
- (18) Burton, A. Enfuvirtide approved for defusing HIV. *Lancet Infect. Dis.* **2003**, *3*, 260.
- (19) Munch, J.; Standker, L.; Adermann, K.; Schulz, A.; Schindler, M.; Chinnadurai, R.; Pohlmann, S.; Chaipan, C.; Biet, T.; Peters, T.; Meyer, B.; Wilhelm, D.; Lu, H.; Jing, W.; Jiang, S.; Forssmann, W. G.; Kirchhoff, F. Discovery and optimization of a natural HIV-1 entry inhibitor targeting the gp41 fusion peptide. *Cell* **2007**, *129*, 263–275.
- (20) Boggiano, C.; Jiang, S.; Lu, H.; Zhao, Q.; Liu, S.; Binley, J.; Blondelle, S. E. Identification of a D-amino acid decapeptide HIV-1 entry inhibitor. *Biochem. Biophys. Res. Commun.* **2006**, *347*, 909–915.
- (21) Smith, J. M.; Ellenberger, D.; Butera, S. Protein Engineering for HIV Therapeutics. In *Medicinal Protein Engineering*; Khudyakov, Y. E., Ed.; CRC Press: Boca Raton, FL, 2009; pp 385–406.
- (22) Herrera, E.; Gómara, M. J.; Mazzini, S.; Ragg, E.; Haro, I. Synthetic peptides of hepatitis G virus (GBV-C/HGV) in the selection of putative peptide inhibitors of the HIV-1 fusion peptide. *J. Phys. Chem. B* **2009**, *113*, 7383–7391.
- (23) Hopp, T. P.; Woods, K. R. Prediction of protein antigenic determinants from amino acid sequences. *Proc. Natl. Acad. Sci. U.S.A.* **1981**, *78*, 3824–3828.
- (24) Janin, J. Surface and inside volumes in globular proteins [20]. *Nature* **1979**, *277*, 491–492.
- (25) Chou, P. Y.; Fasman, G. D. Prediction of the secondary structure of proteins from their amino acid sequence. *Adv. Enzymol. Relat. Areas Mol. Biol.* **1978**, *47*, 45–148.
- (26) Schön, A.; Madani, N.; Klein, J. C.; Hubicki, A.; Ng, D.; Yang, X.; Smith, A. B.; Sodroski, J.; Freire, E. Thermodynamics of binding of a low-molecular-weight CD4 mimetic to HIV-1 gp120. *Biochemistry* **2006**, *45*, 10973–10980.
- (27) Naider, F.; Anglister, J. Peptides in the treatment of AIDS. *Curr. Opin. Struct. Biol.* **2009**, *19*, 473–482.
- (28) Doms, R. Beyond receptor expression: the influence of receptor conformation, density and affinity in HIV-1 infection. *Virology* **2000**, *276*, 229–237.
- (29) Rusert, P.; Mann, A.; Huber, M.; von Wyl, V.; Gunthard, H. F.; Trkola, A. Divergent effects of cell environment on HIV entry inhibitory activity. *AIDS* **2009**, *23*, 1319–1327.
- (30) Nattermann, J.; Nischalke, H. D.; Kupfer, B.; Rockstroh, J.; Hess, L.; Sauerbruch, T.; Spengler, U. Regulation of CC chemokine receptor 5 in hepatitis G virus infection. *AIDS* **2003**, *17*, 1457–1462.
- (31) Wexler-Cohen, Y.; Shai, Y. Demonstrating the C-terminal boundary of the HIV 1 fusion conformation in a dynamic ongoing fusion process and implication for fusion inhibition. *FASEB J.* **2007**, *21*, 3677–3684.
- (32) Derdeyn, C. A.; Decker, J. M.; Sfakianos, J. N.; Wu, X.; O'Brien, W. A.; Ratner, L.; Kappes, J. C.; Shaw, G. M.; Hunter, E. Sensitivity of human immunodeficiency virus type 1 to the fusion inhibitor T-20 is modulated by coreceptor specificity defined by the V3 loop of gp120. *J. Virol.* **2000**, *74*, 8358–8367.
- (33) Derdeyn, C. A.; Decker, J. M.; Sfakianos, J. N.; Zhang, Z.; O'Brien, W. A.; Ratner, L.; Shaw, G. M.; Hunter, E. Sensitivity of human immunodeficiency virus type 1 to fusion inhibitors targeted to the gp41 first heptad repeat involves distinct regions of gp41 and is consistently modulated by gp120 interaction with the coreceptor. *J. Virol.* **2001**, *75*, 8605–8614.
- (34) Gordon, L. M.; Mobley, P. W.; Pilpa, R.; Sherman, M. A.; Waring, A. J. Conformational mapping of the N-terminal peptide of HIV-1 gp41 in membrane environments using <sup>13</sup>C-enhanced Fourier transform infrared spectroscopy. *Biochim. Biophys. Acta* **2002**, *1559*, 96–120.
- (35) Garcia-Martin, F.; Quintanar-Audelo, M.; Garcia-Ramos, Y.; Cruz, L. J.; Gravel, C.; Furic, R.; Cote, S.; Tulla-Puche, J.; Albericio, F. ChemMatrix, a poly(ethylene glycol)-based support for the solid-phase synthesis of complex peptides. *J. Comb. Chem.* **2006**, *8*, 213–220.
- (36) Garcia-Martin, F.; White, P.; Steinauer, R.; Cote, S.; Tulla-Puche, J.; Albericio, F. The synergy of ChemMatrix resin and pseudoproline building blocks renders RANTES, a complex aggregated chemokine. *Biopolymers* **2006**, *84*, 566–575.
- (37) Ellens, H.; Bentz, J.; Szoka, F. C. pH-induced destabilization of phosphatidylethanolamine-containing liposomes: role of bilayer contact. *Biochemistry* **1984**, *23*, 1532–1538.
- (38) Larios, C.; Casas, J.; Alsina, M. A.; Mestres, C.; Gomara, M. J.; Haro, I. Characterization of a putative fusogenic sequence in the E2 hepatitis G virus protein. *Arch. Biochem. Biophys.* **2005**, *442*, 149–159.
- (39) Rojo, N.; Gomara, M. J.; Alsina, M. A.; Haro, I. Lipophilic derivatization of synthetic peptides belonging to NS3 and E2 proteins of GB virus-C (hepatitis G virus) and its effect on the interaction with model lipid membranes. *J. Pept. Res.* **2003**, *61*, 318–330.
- (40) Wimley, W. C.; White, S. H. Designing transmembrane alpha-helices that insert spontaneously. *Biochemistry* **2000**, *39*, 4432–4442.
- (41) Sackett, K.; Wexler-Cohen, Y.; Shai, Y. Characterization of the HIVN-terminal fusion peptide-containing region in context of key gp41 fusion conformations. *J. Biol. Chem.* **2006**, *281*, 21755–21762.
- (42) Wei, X. P.; Decker, J. M.; Liu, H. M.; Zhang, Z.; Arani, R. B.; Kilby, J. M.; Saag, M. S.; Wu, X. Y.; Shaw, G. M.; Kappes, J. C. Emergence of resistant human immunodeficiency virus type 1 in patients receiving fusion inhibitor (T-20) monotherapy. *Antimicrob. Agents Chemother.* **2002**, *46*, 1896–1905.
- (43) Nussbaum, O.; Broder, C. C.; Berger, E. A. Fusogenic mechanisms of enveloped-virus glycoproteins analyzed by a novel recombinant vaccinia virus-based assay quantitating cell fusion-dependent reporter gene activation. *J. Virol.* **1994**, *68*, 5411–5422.
- (44) Ratkowsky, D. A. *Handbook of Nonlinear Regression Models*; Dekker: New York, 1990; Vol. 107, p 241.